Original Article

Development and characterization of neural network-based multianalyte delta checks

Christopher R. Jackson, Mark A. Cervinski

Department of Pathology and Laboratory Medicine, Dartmouth-Hitchcock Medical Center, Lebanon, NH, USA

Contributions: (I) Conception and design: CR Jackson; (II) Administrative support: MA Cervinski; (III) Provision of study materials or patients: MA Cervinski; (IV) Collection and assembly of data: All authors; (V) Data analysis and interpretation: All authors; (VI) Manuscript writing: All authors; (VII) Final approval of manuscript: All authors.

Correspondence to: Christopher R. Jackson, MD. Department of Pathology and Laboratory Medicine, Dartmouth-Hitchcock Medical Center, Lebanon, NH 03756, USA. Email: Christopher.R.Jackson@hitchcock.org.

Background: In laboratory medicine, mislabeled specimens (MLS) are pre-analytical errors where a tube of blood is given the wrong patient ID. When pre-analytical methods fail to catch these errors, post-analytical methods are employed to identify MLS. Inspired by delta checks, we employed neural networks to create a variety of novel algorithms aimed to detect MLS. In this approach, the neural networks evaluate the analytical results from two different time points to determine if they belong to the same patient.

Methods: Raw analytical data was collected from clinical practice. Analytes were grouped by patient and collection time, and groups of specimens were linked to create a dataset of properly labeled specimen pairs. The data was processed to simulate MLS by reassigning the second set of analytes to a different patient. In one approach, neural networks were created where both groups of analytes were set panels [e.g., basic metabolic panels (BMP) or comprehensive metabolic panels (CMP)]. In a second approach, neural networks were created where the groups of analytes could consist of any combination of analytes. For both approaches, different neural networks were created for different ranges of time-deltas, and these were evaluated using receiver operator characteristics curve analysis. The performance of each neural network was compared to the current delta check strategy used at our institution.

Results: The best performing neural network was the one that compared analytical results from CMPs for time-deltas <1.5 days. This achieved an area under the curve (AUC) of 0.994 and significantly outperformed the classic delta check methods. The best performing open neural network achieved an AUC of 0.964 when 13 analytes were used time deltas <1.5 days.

Conclusions: The implementation of machine learning-based protocols to detect MLS with fewer false-positive errors may have a dramatic impact on patient care and health care costs.

Keywords: Neural network; delta check; machine learning; mislabeled specimen (MLS)

Received: 14 February 2020; Accepted: 16 March 2020; Published: 20 April 2020.

doi: 10.21037/jlpm.2020.02.03

View this article at: http://dx.doi.org/10.21037/jlpm.2020.02.03

Introduction

In laboratory medicine, mislabeled specimens (MLS) are pre-analytical errors where blood from one patient is given an ID label from a different patient. These errors are estimated to occur in between 0.03 to 17 specimens per 1000 specimens collected (1-4). It is likely that the lower estimates may be falsely low due to the difficulty in identifying these errors in clinical practice. When MLS are not detected, they can place one or both patients at risk of harm as clinical decisions are carried out based on incorrect data. MLS are estimated to cost 280,000 USD per million specimens collected, and cause 160,000 adverse medical events per year in the United States (5).

Pre-analytical solutions have been relatively successful at reducing the number of MLS. In one study, the implementation of barcode labels with bedside printers reduced the number of MLS by 92% (6). In a multi-institutional survey, MLS were noted to occur significantly less frequently in institutions with ongoing quality monitoring systems for specimen identification, and in institutions with 24/7 inpatient phlebotomy service (3). One approach to reducing MLS is to give patients identifying wristbands, but wristband errors can result in downstream MLS error. To reduce the number of wristband errors, the College of American Pathologists performed a study involving 217 institutions where phlebotomists were tasked with continuously evaluating patient wristbands for error. This strategy reduced wristband errors from 7.40% to 3.05% (7).

In cases where pre-analytical strategies fail, post-analytical methods to detect MLS have been developed. *Delta checks* are one such system and are widely used due to the low cost of implementation. In this method, patients' analytical test results from two different time points are compared. If the value change exceeds a pre-determined threshold, the results are flagged and either reviewed, repeated, or the specimen is recollected (8). Multiple strategies using this framework have been implemented. Thresholds, for example, can be applied to the absolute change in value (current result minus the previous result), or a relative change in value (current result divided by the previous result). Change velocities (change in value divided by the difference in collection time) can also be used. No standard acceptable tolerances have been established, although median values have been reported (8). Despite widespread implementation of delta-checks in clinical laboratories, the value of this strategy is questionable. Receiver operator characteristics curve (ROC) analysis has shown that the best performing delta check was for mean corpuscular volume (MCV) which only achieved an area under the curve (AUC) of 0.90 (9). In one analysis, multiple analytes were combined and a weighted cumulative delta check was implemented. Although this model achieved promising results with a maximum AUC of 0.98 (10), the same data was used to both generate and test their model, introducing a significant source of potential bias.

Recently, delta checks were revisited using machine learning techniques. An AUC of 0.97 was achieved using a support vector machines (SVM) method (11), showing that a better performance could be achieved as compared logistical regression (AUC =0.92). Despite their achievement, the researchers limited their analysis to a rigid panel of 11 analytes, and only examined specimens collected within 36 hours of one another. This restrictive approach likely meant that only a small minority of all the blood-specimens collected at their institution could be evaluated by their model. Although they compared their method to a weighted logistical regression model, these were also limited to the same 11 analytes as their SVM method, even if more tests were actually performed.

To expand and improve upon previous work, we devised two novel machine learning methods to identify MLS using neural networks. In one approach, the results from rigid analyte panels were used to identify MLS. In the second approach, neural networks were created that were not limited to a specific panel of analytes, but instead could be given any combination of analytes. For both approaches, different neural networks were created and evaluated for different ranges of time deltas. The performance of each neural network was compared directly to the current delta check strategy used at our institution.

Methods

Data processing

A MatLab code was created to automate all data processing, and to create and test all neural networks. MATLAB R2018b (MathWorks, version 9.5.0.944444, Natick, Massachusetts, USA) was used.

Datasets

All analytical test results performed on our automated core chemistry and immunoassay analyzers at our institution between 4/12/2012 to 1/30/2014 (1.8 years) were collected. All patient medical record numbers were de-identified via assignment of unique numeric codes that were not tied to the original numbers. The complete list of analytical tests is shown in *Table S1*. The test results were sorted by patient and time of collection, and bundled with all other test results from the same patient that were collected at the same time (*Figure 1A*). A total of 4,119,977 analytical tests from 122,433 patients over 462,998 unique time points were obtained. Test-bundles with less than 5 analytes were discarded from the set.

Combinations of two test-bundles from a single patient were linked to create properly-labeled-specimen-pairs

A

Time Bundles

	Patient	Time point	Time point A		
			Result 1 (Na)	Result 2 (K)	...
Test-bundle 1:	1	4/12/2012 1 AM	138.3	4.2	
Test-bundle 2:	1	4/13/2012 2 AM	139.5	4.2	
Test-bundle 3:	1	4/14/2012 1 AM	137.1	3.9	

B

Properly-labeled specimen pairs

Patient	First time point			Second time point			Δt[days]
	Result 1(Na)	Result 2(K)	...	Result 1 (Na)	Result 2 (K)	...	
1	138.3	4.2		139.5	4.3		1.1
1	139.5	4.3		140.1	4.1		2.1
2	137.1	3.9		140.0	4.0		0.9
2	140.0	3.9		140.9	3.8		1.6
3	142.3	4.6		141.8	4.7		0.9
3	141.8	4.7		141.5	4.5		6.2

C

Mislabeled specimen pairs

Patient	First time point			Second time point			Δt[days]
	Result 1(Na)	Result 2(K)	...	Result 1 (Na)	Result 2 (K)		
1	138.3	4.2		140.3	5.2		1.1
1	139.5	4.3		141.3	5.1		2.1
2	137.1	3.9		139.5	4.3		0.9
2	140.0	3.9		140.1	4.1		1.6
3	142.3	4.6		140.0	4.0		0.9
3	141.8	4.7		140.9	3.8		6.2

D

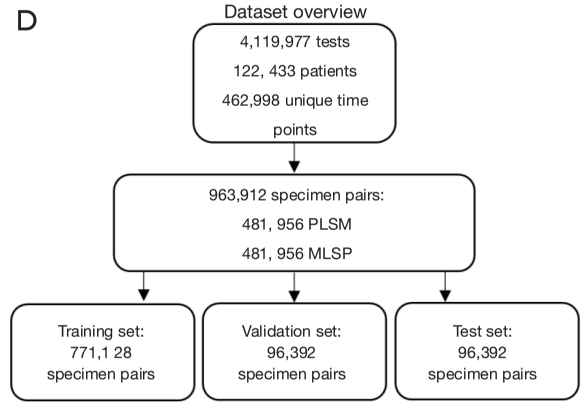

E

Layers	Types	Size
1	Input layer	(N+1) x4x 1
2-5	Convolution (1), Batch normalization (1), ReLU (1)	15X4x8
6-9	Convolution (2), Batch normalization (2), ReLU (2)	7x2X16
10-13	Convolution (3), Batch normalization (3), ReLU (3)	4x1X32
14-17	Convolution (4), Batch normalization (4), ReLU (4)	2x1x32
18	Fully connected layer	1x1x2
19	Softmax	1x1x2
20	Classification output	1x1x2

F

$[A_1, t_1]$	$[A_2, t_1]$	$[A_3, t_1]$	...	$[A_N, t_1]$	Δt
$[A_1, t_2]$	$[A_2, t_2]$	$[A_3, t_2]$	...	$[A_N, t_2]$	0
$[A_1, t_1]$-$[A_1, t_2]$	$[A_2, t_1]$-$[A_2, t_2]$	$[A_3, t_1]$-$[A_3, t_2]$	...	$[A_N, t_1]$-$[A_N, t_2]$	0
$[A_1, t_1]$/$[A_1, t_2]$	$[A_2, t_1]$/$[A_2, t_2]$	$[A_3, t_1]$/$[A_3, t_2]$	...	$[A_N, t_1]$/$[A_N, t_2]$	0

Figure 1 Analytical test results were assembled and sorted by patient and by time of specimen collection. All test results for a single patient at a single time point were grouped into a test-bundle (A). Test-bundles were then linked to other test-bundles from the same patient to create a set of properly-labeled-specimen-pairs (PLSP) (B). Mislabeled specimen pairs were then simulated by reassigning the second test-bundle in the PLSP to a different patient (C). The PLSP and MLSP were then randomly assigned to a training set, validation set, and test set (D). The neural networks consisted of 20 layers (E), the last layer being an output classification layer (PLSP vs. MLSP). The input layer consisted of the analytical test results from specimen pairs ([A1,t1], [A1,t2], [A2,t1], [A2,t2],...[An,t2]), along with the time between specimen collection, Δt (F).

Table 1 Analytes within each panel

Panel name	Analytes
Basic metabolic panel (BMP)	Na, K, Cl, CO2, BUN, CRE, GLUC, Ca
Comprehensive metabolic panel (CMP)	Na, K, Cl, CO2, BUN, CRE, GLUC, Ca, ALKP, ALT, AST, TBILI, TP, ALB
Hepatic function panel (HFP)	ALKP, ALT, AST, ALB, TBILI, DBILI, TP
Renal function panel (RFP)	Na, K, Cl, CO2, BUN, CRE, GLUC, Ca, ALB, PHOS

ALB, albumin; ALKP, alkaline phosphatase; ALT, alanine aminotransferase; AST, aspartate aminotransferase; BUN, blood urea nitrogen; CA, calcium; CL, chloride; CO2, bicarbonate; CRE, creatinine; DBILI, direct bilirubin; GLUC, glucose; K, potassium; NA, sodium; PHOS, phosphorus; TBILI, total bilirubin; TP, total protein.

(PLSP) (*Figure 1B*). Every possible combination was produced, and the time between each linked pair was recorded. The delta time, Δt, is the time difference between two collection times:

$\Delta t = t_B - t_A$

where t_A and t_B are the first and second time points. PLSP with a Δt greater than 10 days were discarded from the dataset.

Mislabeled specimen simulation

Mislabeled-specimen-pairs (MLSP) were created by randomly reassigning the analytical test results from the second time point to a different patient (*Figure 1C*). Test-bundles were always reassigned to different patients that had the same set of analytes performed. In cases where there were insufficient unique patients to reassign the test results to a different patient, both the MLSP and corresponding PLSP were discarded. A total of 481,956 PLSP and MLSP (963,912 pairs in total) were created in this manner, spanning 18,886 patients. 80% of the specimen-pairs (771,128 pairs) were randomly assigned to a master-training set, while 10% (96,392 pairs) each were assigned to a validation set and a test set (*Figure 1D*). The data sets were then divided into five groups depending on their Δt: <1.5, 1.5–2.5, 2.5–3.5, 3.5–5, and 5–10 days.

Neural networks were created to predict if specimen-pairs were PLSP or MLSP using different methodologies described below.

Panel neural networks (PNN)

PNN were created to detect MLS when the same panel was ordered at two time points. All analytes that were not in the panels were discarded for this analysis. Specimen pairs that did not have the full panel were likewise discarded. The panels that were evaluated included the basic metabolic panel (BMP), the comprehensive metabolic panel (CMP), the renal function panel (RFP), and the liver function panel (LFP). Analytes for each panel are listed in *Table 1*, while the number of specimen pairs used to train, validate, and test each PNN are shown in *Table S2*, along with neural network training parameters.

The prototypical neural network architecture is shown in *Figure 1E*, and the prototypical input layer is shown in *Figure 1F*. In brief, the input layer was an (N+1)×4 matrix, where N is the number of analytes in the test-panel. The first N columns each correspond to a different analyte. The first row was populated with the analytes from the first time-point, while the second row was populated with the analytes from the second time point. The third row was populated with the absolute change in value between the two time points (current result minus the previous result), while the fourth row was populated by the relative change in value (current result divided by the previous result). The cell in row 1 of the final column (column N+1) was populated by Δt in days, while cells in rows 2, 3, and 4 in the final column were left as 0. The PNNs were trained between 20 and 100 epochs each. Ten PNNs were created for each panel and for each group of Δt ranges in order to perform statistical analysis.

Open-ended neural networks (ONN)

ONN were created to detect MLS regardless of what tests were ordered at either time point. For these networks, the data sets were separated based on the number of analytes ordered at the second time point. The specimen pair data was thus divided into three groups: group 1 (5 to 8 analytes tested at the second time-point), group 2 (9 to 12 analytes), and group 3 (13 or more analytes). The number of analytical tests performed at the first time point did not affect what category the specimen pair was placed in. Likewise, the same analytes did not need to be ordered at both time points in the specimen pair. The number of

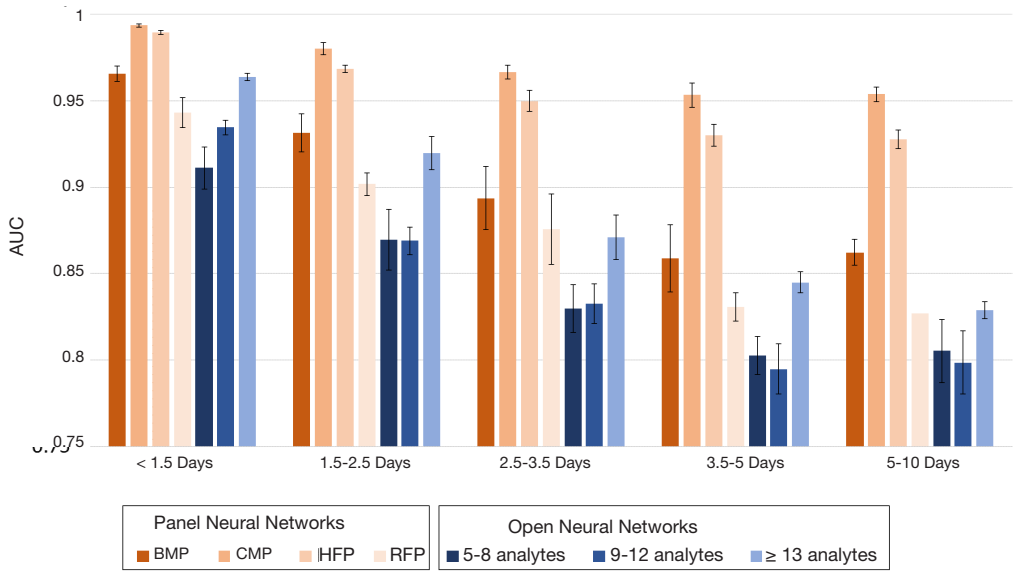

Figure 2 Area under the curve (AUC) results for the neural networks generated from the receiver operator characteristics curve (ROC) analysis. The basic metabolic panel (BMP), comprehensive metabolic panel (CMP), hepatic function panel (HFP) and renal function panel (RFP) were all assessed by panel neural networks (PNN). The 5–8, 9–12, and ≥13 analyte protocols were all assessed by open neural network (ONN).

specimen pairs used to train, validate, and test each ONN are shown in *Table S2*, along with neural network training parameters.

The structure for the ONNs is similar to that of the PNNs. The difference between the approaches was in the input layer, which consisted of a 131×4 matrix. The first 130 columns either corresponded to different analytes, or was left blank (assigned a value of zero). Similar to PNNs, the first row corresponded to the value at the first time point, the second row corresponded to the value at the second time point, the third row corresponded to the absolute change in value, and the fourth row corresponded to the relative change in value. When an analyte was not tested at a given time-point, that column was left as zero. When an analyte was only tested at the first time point and not at the second time point, row 1 was populated with the test result, and rows 2, 3, and 4 were left as zero. Similarly, when an analyte was only tested at the second time point and not the first, row 2 was populated with the result and rows 1, 3 and 4 were left as zero.

Similar to PNNs, for ONNs, the cell in the first row of the final column (column 131) was populated by Δt in days, while cells in rows 2, 3, and 4 of the final column were set to zero. The ONNs were trained between 20 and 100 epochs each. Ten ONNs were created for each panel and for each group of Δt ranges for statistical analysis.

Statistical analysis

ROC analysis was performed for each neural network using the PLSP and MLSP categories as the gold standard, and the neural network output score as the analyte. The AUC was calculated for each neural network. The sensitivity and specificity were obtained for the optimal operating point (OOP) on the ROC curve as calculated by the MATLAB *perfcurve* function that relies on a previously described cost-function curve analysis (12). The specificity was also calculated for each neural network at the points where the sensitivities reached 50% and 80%. A positive predictive value (PPV) was calculated assuming a mislabeled-specimen frequency of 1 in 200 (0.5%). This was performed for the OOP, as well as at the points where the sensitivities were set to 50% and 80%. Neural networks performance metrics are reported as mean ± standard deviation.

Classic delta checks

The data sets used to test the PNNs and ONNs were also evaluated using the classic delta check limits used at our institution. Classic delta check limits were derived from

reference change limit calculations and can be viewed in *Table S1*. In order to properly compare the two methods, the classic delta checks were applied to all analytes that were performed at both time points in the specimen pairs. For the PNNs, analytes that were not in a given panel were still included in the classic delta check analysis. The number of times each test was ordered in our cohort, and the mean and standard deviation change over the course of 1.5 days are described in *Table S1*. The PPVs for each PNN and ONN test set were calculated using the classic delta checks.

Results

ROC analysis

ROC analysis was applied to all neural networks. The mean AUCs for all the neural networks are compiled in *Figure 2* and listed in *Table S3*. The best performing neural network was the CMP PNN for Δt <1.5 days, which achieved an AUC of 0.994±0.001. The CMP neural networks were the best performing of all neural networks, maintaining an AUC above 0.95 even for the 5 to 10 day Δt. The HPF PNNs were the second best performing PNNs, the BMP PNNs were third, and the RFP PNNs were fourth. In general, the ONNs performed similar to or worse than the PNNs. Performance in the ONNs improved as the number of test-analytes increased. In general, both PNNs and ONNs with low Δt performed best, and performance decreased as the Δt increased.

Sensitivity and specificity analysis

The sensitivities, specificities, and PPVs are shown for the PNNs and the ONNs in *Tables S4* and *S5*, respectively. PNN results are shown in *Figure 3*, while the ONN results are shown in *Figure 4*. Similar to the AUC values, sensitivity and specificity generally decreased as the Δt increased. The CMP PNN with a Δt of <1.5 days had the highest OOP sensitivity and specificity which were 98.4% and 96.4% respectively. When sensitivities were set to 50%, the specificities for the CMP PNNs were all in excess of 99.4% regardless of the Δt. These additionally had PPVs greater than 29% for all time periods when a 0.5% MLSP frequency was assumed. The PPVs for the CMP PNNs with Δt <1.5 days and 1.5 to 2.5 days were both greater than 68%, however, these groups each represent less than 1% of the total specimen pairs. Although the BMP PNN with Δt <1.5 days had a smaller PPV (41.7%), this neural network covers a much larger proportion of all the specimen pairs (19.3%).

For the ONN, when sensitivity was set to 50%, only the 13-analyte ONN with a Δt <1.5 days had a specificity that exceeded 99% (actual value =99.5%), which resulted in a PPV of 17.6%.

The classic delta checks were highly sensitive in identifying MLSPs, but their specificities were lower than all the neural networks at the OOP. When classic delta checks were evaluated on the panel data sets, the highest PPV achieved was 1.7% for the BMP data set with a Δt <1.5 days. The highest PPV achieved using the classic delta checks in the open data sets was 1.9% for the 5–8 analyte data set with a Δt <1.5 days.

Conclusions

Neural networks were created to identify MLS. Using this method, the best AUC achieved was 0.994±0.001 for a CMP PNN with Δt <1.5 days. This study improves upon previous work by increasing the maximum AUC achieved in detecting mislabeled specimen (11). We additionally created neural networks designed to detect MLS when alternative panels were performed, namely BMPs, RFPs, and HFPs. We compared this strategy to an unrestricted approach, where any analyte could be used at either time point. These ONNs were less accurate than the PNNs at detecting MLS, however their flexibility may have some niche applications.

Although the BMP PNN only produced a PPV of 41.7% with a sensitivity of 50%, it is worth highlighting the magnitude of difference in PPV of the PNN when compared to the classic delta checks. The BMP PNN had a 24-fold improvement in PPV when compared to the classic delta checks which had a maximum PPV of 1.7% using the same BMP analytes, though at the sacrifice of sensitivity. The low PPV is in part due to an overly-sensitive classic delta check strategy, which increased both the true-positive rates as well as the false positive rates. A high false positive rate diverts laboratory resources and can become costly to investigate MLS. The analytical tests often need to be repeated, there can be additional blood loss incurred due to the necessity of repeating phlebotomy, and laboratory personnel need to spend time reviewing and analysing the error. The implementation of machine learning-based protocols to detect MLS with fewer false-positive errors may have a dramatic impact on patient care and health care costs, and require little-to-no monetary investment.

One of the strengths and limitations of our study was

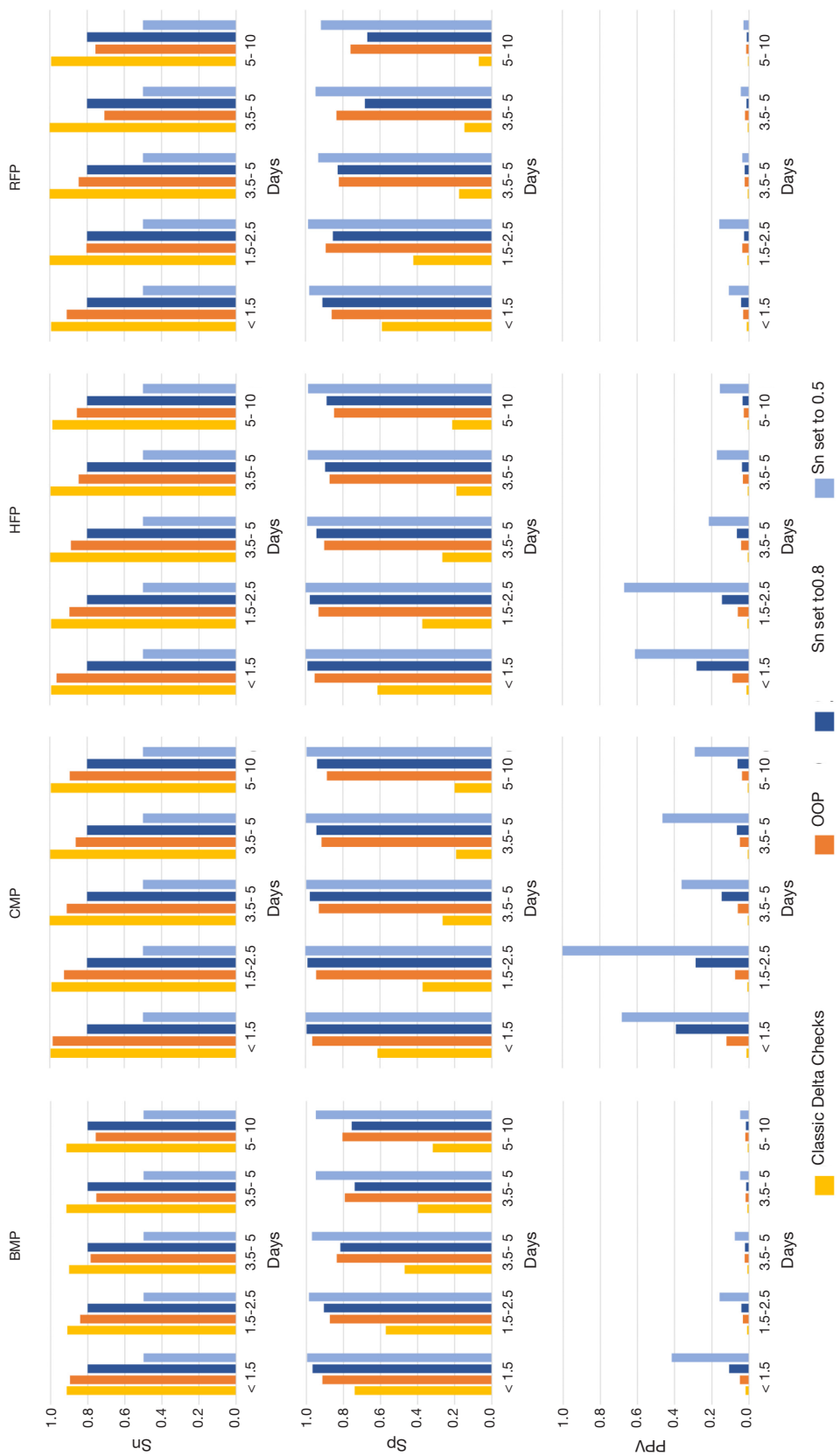

Figure 3 Panel neural network (PNN) results. Sensitivity (Sn), specificity (Sp), and positive predictive values (PPV) for a MLS frequency of 0.5% (1 in 200) for the various panel neural networks (PNN). BMP, basic metabolic panel; CMP, comprehensive metabolic panel; HFP, hepatic function panel; OOP, optimal operating point; RFP, renal function panel; Sn, sensitivity; Sp, specificity.

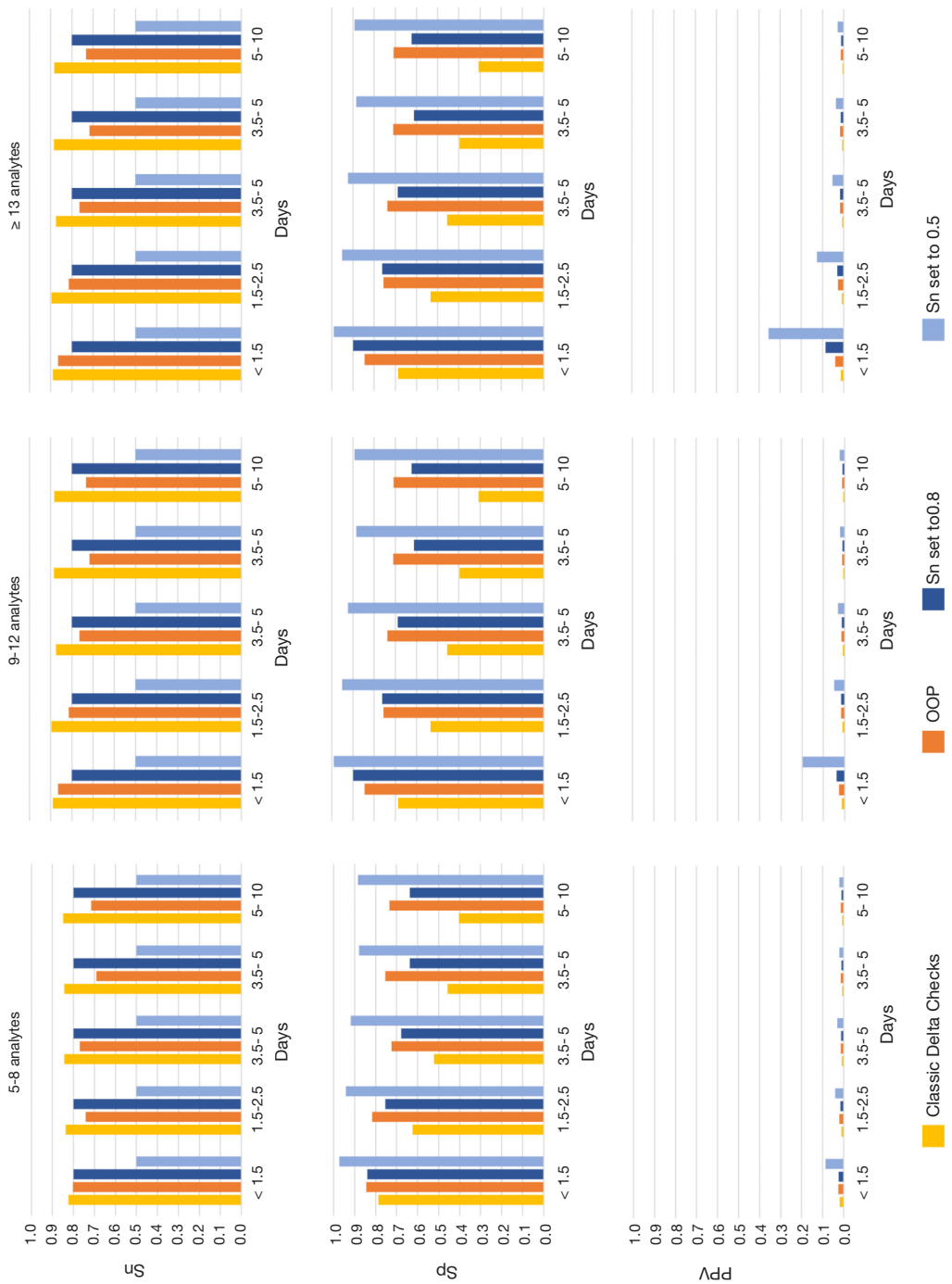

Figure 4 Open neural network results. Sensitivity (Sn), specificity (Sp), and positive predictive values (PPV) for a MLS frequency of 0.5% (1 in 200) for the various open neural networks (ONN). OOP, optimal operating point; Sn, sensitivity; Sp, specificity.

that pre-existing clinical data obtained from our middleware system was utilized. Using pre-existing data, rather than simulated data, allowed for the direct analysis of realistic scenarios in which the blood-in-tube of the MLS sample could come from any random patient. The limitation of this strategy is that undetected MLS were likely present in the raw data, and these were miscategorized as PLSP in the training and test sets. The effect of undetected MLS pairs in our training and test sets would be expected to have decreased the performance and lowered the AUC of the PNNs and ONNs.

Neural networks and other machine learning strategies have clear advantages over conventional classic delta checks, but these should be implemented with caution due to a number of practical limitations. The algorithms typically generate a "black box" approach to error detection which needs to be evaluated empirically. The strategy relies heavily on the use of contemporary clinical data to train the algorithm. The frequency by which new data must be collected and new neural networks must be trained needs to be established.

Finally, the implementation of machine learning based MLS-detection protocols requires a dedicated understanding of rapidly evolving artificial intelligent technologies. Given the demonstration of improved performance of these protocols over the classic delta checks, laboratory information systems and middleware vendors must be pressed to develop software that can utilize these tools in real-time.

Acknowledgments

The research project was possible due to the generous donation of an Nvidia Titan XP graphics processing unit as part of the GPU Research Grant (Nvidia, Santa Clara, California). In addition, this work was supported by the Dartmouth Hitchcock Medical Center Department of Pathology and Laboratory Medicine.

Footnote

Provenance and Peer Review: This article was commissioned by the editorial office, *Journal of Laboratory and Precision Medicine* for the series "Patient Based Quality Control". The article has undergone external peer review.

Conflicts of Interest: Both authors have completed the ICMJE uniform disclosure form (available at http://dx.doi.org/10.21037/jlpm.2020.02.03). The series "Patient Based Quality Control" was commissioned by the editorial office without any funding or sponsorship. Mark Cervinski served as an unpaid Guest Editor of the series and serves as an unpaid editorial board member of *Journal of Laboratory and Precision Medicine* from May 2019 to April 2021. Dr. Jackson reports that the GPU used to perform the research was donated to him by NVIDIA as part of the NVIDIA GPU grant program.

Ethical Statement: The authors are accountable for all aspects of the work in ensuring that questions related to the accuracy or integrity of any part of the work are appropriately investigated and resolved. The institutional review board (IRB) at our institution determined that the project is not research involving human subjects as defined by our internal and FDA regulations. IRB review and approval by the organization is not required. The outcomes of the study will not affect the future management of the patients involved.

References

1. Dzik WH, Murphy MF, Andreu G, et al. An international study of the performance of sample collection from patients. Vox Sang 2003;85:40-7.
2. Ansari S, Szallasi A. "Wrong blood in tube": Solutions for a persistent problem. Vox Sang 2011;100:298-302.
3. Wagar EA, Stankovic AK, Raab S, et al. Specimen labeling errors: A Q-probes analysis of 147 clinical laboratories. Arch Pathol Lab Med 2008;132:1617-22.
4. Saathoff AM, MacDonald R, Krenzischek E. Effectiveness of Specimen Collection Technology in the Reduction of Collection Turnaround Time and Mislabeled Specimens in Emergency, Medical-Surgical, Critical Care, and Maternal Child Health Departments. Comput Inform Nurs 2018;36:133-9.
5. Valenstein PN, Raab SS, Walsh MK. Identification errors

involving clinical laboratories: A College of American Pathologists Q-Probes study of patient and specimen identification errors at 120 institutions. Arch Pathol Lab Med 2006;130:1106-13.
6. Brown JE, Smith N, Sherfy BR. Decreasing Mislabeled Laboratory Specimens Using Barcode Technology and Bedside Printers. J Nurs Care Qual 2011;26:13-21.
7. Howanitz PJ, Renner SW, Walsh MK. Continuous wristband monitoring over 2 years decreases identification errors: A College of American Pathologists Q-Tracks study. Arch Pathol Lab Med 2002;126:809-15.
8. Schifman RB, Talbert M, Souers RJ. Delta check practices and outcomes a q-probes study involving 49 health care facilities and 6541 delta check alerts. Arch Pathol Lab Med 2017;141:813-23.
9. Balamurugan S, Rohith V. Receiver Operator Characteristics (ROC) Analyses of Complete Blood Count (CBC) Delta. J Clin DIAGNOSTIC Res 2019;13:9-11.
10. Yamashita T, Ichihara K, Miyamoto A. A novel weighted cumulative delta-check method for highly sensitive detection of specimen mix-up in the clinical laboratory. Clin Chem Lab Med 2013 51:781-9.
11. Rosenbaum MW, Baron JM. Using machine learning-based multianalyte delta checks to detect wrong blood in tube errors. Am J Clin Pathol 2018;150:555-66.
12. Zweig MH, Campbell G. Receiver-operating characteristic (ROC) plots: A fundamental evaluation tool in clinical medicine. Clin Chem 1993;39:561-77.

doi: 10.21037/jlpm.2020.02.03
Cite this article as: Jackson CR, Cervinski MA. Development and characterization of neural network-based multianalyte delta checks. J Lab Precis Med 2020;5:10.

Supplementary

Table S1 Characterization of test analytes

Analyte	Abbreviation	Number of tests	Test pairs			Units	Classic strategy	
			N pairs with Δt <1.5 days	Absolute change (mean +/− SD)	Relative change (mean +/− SD)		Threshold	Absolute vs. relative
Thyroid stimulating hormone	TSH	97,125	128	0.23±2.39	1.15±0.71	mcIU/mL	1	R
Thyroxine	T4	4,453	12	−0.30±1.21	0.980±0.083	ng/dL	1	R
Free thyroxine	FREE T4	20,156	37	0.157±0.494	1.09±0.25	mcg/dL	–	None
Triiodothyronine	T3Q	3,509	26	24.9±69.3	1.24±0.49	pg/mL	0.3	R
T-uptake	TUP	1,131	3	0.0073±0.0481	1.01±0.060	Ratio	0.25	R
Estradiol	E2	2,705	0	–	–	pg/mL	–	None
Testosterone	TSTO	3,556	0	–	–	ng/mL	–	None
Prolactin	PROLAC	2,571	1	−1.73±0	0.858±0	ng/mL	–	None
Progesterone	PROGEST	638	0	–	–	ng/mL	–	None
Total bilirubin	TBILI	151,747	8,982	−0.04±1.21	1.09±0.47	mg/dL	0.75	R
Luteinizing hormone	LH	1,569	0	–	–	mIU/mL	–	None
Follicle stimulating hormone	FSH	2,978	0	–	–	mIU/mL	–	None
Cortisol	CORT	2,802	69	0.3±10.7	1.29±1.40	mcg/dL	–	None
High density lipoprotein cholesterol	HDL	93,934	32	0.16±3.15	1.01±0.09	mg/dL	–	None
Troponin T	CTNT	10,182	2,339	−0.24±2.89	1.00±0.84	ng/mL	0.5	A
L-lactate	LLACT	12,053	6,360	0.57±1.90	1.46±0.94	mmol/L	0.5	R
Carcinoembryonic antigen	CEA	1,002	0	–	–	ng/mL	–	None
Prostate specific antigen	PSA	16,183	5	−2.32±5.25	1.04±0.11	ng/mL	–	None
Creatine phosphokinase	CPK	31,573	6,520	−30±2180	1.19±0.76	U/L	0.75	R
Ferritin	FERRI	14,633	9	−14.1±39.6	0.979±0.234	ng/mL	–	None
Lactate dehydrogenase	LDH	2,335	165	−145±686	1.10±0.68	U/L	0.9	R
Pro B-type natriuretic peptide	PROBNP	6,693	83	460±4740	1.07±0.47	pg/mL	–	None
Vitamin B12	B12	14,068	6	−26±187	1.00±0.16	pg/mL	–	None
folate, serum	S FOLATE	5,888	4	0.815±1.72	1.10±0.20	ng/mL	1	R
urine protein	U Prot	3,208	1	74.0±0	3.85±0	g/24 hrs	–	None
human chorionic gonadotropin	HCG	5,524	1	−61.2±0	0.685±0	mIU/mL	–	None
alkaline phosphatase	ALKP	151,745	8,914	3.6±46.8	1.04±0.22	U/L	0.7	R
High sensitivity C-reactive protein	HSCRP	21,555	90	27.7±78.0	1.67±2.58	mg/L	–	None
Beta-hydroxybutyrate	BOHB	809	513	0.97±2.10	5.8±17.8	mmol/L	–	None
Albumin	ALB	155,262	9,162	0.080±0.379	1.03±0.15	g/dL	0.3	R
Rheumatoid factor	RF	4,324	0	–	–	IU/mL	–	None
Acetaminophen	ACAM	138	14	48.1±75.8	9.23±8.66	mg/L	–	None
Blood urea nitrogen	BUN	285,912	113,112	0.92±7.41	1.09±0.36	mg/dL	0.6	R
Urine urea nitrogen	U UREA	593	5	19.8±258	1.37±0.84	g/24 hrs	–	None
Total cholesterol	CHOL	94,742	38	10.2±38.2	1.05±0.14	mg/dL	0.3	R
Bicarbonate	CO2	288,534	119,059	−0.30±2.87	0.993±0.140	mmol/L	0.5	R
Ammonia	AMON	1,733	78	11.1±50.8	1.28±0.73	mcmol/L	1	R
Gamma glutamyl transferase	GGT	1,123	1	1±0	1.2±0	U/L	0.55	R
Amylase	AMY	4,531	450	44±182	1.21±0.49	U/L	0.75	R
Direct bilirubin	DBILI	149,189	7,807	−0.011±0.789	1.12±0.58	mg/dL	0.75	R
Iron	IRON	11,867	22	1.43±8.82	1.03±0.21	mcU/dL	–	None
Total protein	TP	152,787	8,826	0.146±0.626	1.03±0.12	g/dL	0.3	R
Alanine aminotransferase	ALT	156,572	8,571	4±292	1.08±0.37	U/L	0.8	R
Aspartate aminotransferase	AST	156,583	8,147	16±377	2.7±99.3	U/L	0.8	R
Magnesium	MG	42,159	24,722	−0.009±0.132	0.997±0.174	mmol/L	0.5	R
Urine magnesium	U MG	50	1	0.88±0	1.378±0	mmol/L	–	None
Uric acid	URIC	6,066	334	0.18±1.46	1.13±0.92	mg/dL	0.5	R
Uric acid, urine	U URIC	80	0	–	–	g/24 hrs	–	None
Ethanol	ETOH	2,403	19	1530±1270	278±909	mg/L	–	None
Calcium	CA	264,544	103,280	0.008±0.546	1.00±0.07	mg/dL	0.1	R
Urine calcium	U CA	395	0	–	–	mg/24 hrs	–	None
Phosphorus	PHOS	30,784	18,717	0.04±1.08	1.06±0.49	mg/dL	0.8	R
Urine phosphorus	U PHOS	102	0	–	–	mg/dL	–	None
Lipase	LIPA	9,099	693	86±528	1.56±1.87	U/L	0.75	R
Glucose	GLUC	292,116	108,102	7.2±61.6	1.09±0.44	mg/dL	1.6	R
Creatinine	CRE	291,889	111,619	0.061±0.463	1.07±0.46	mg/dL	0.8	A
Urine creatinine	UCRE RAN	19,497	9	17.4±61.3	1.54±1.16	mg/dL	–	None
Salicylate	SALI	146	15	114±112	50.5±99.5	mg/L	–	None
Triglyceride	TRIG	90,779	76	65±267	1.14±0.54	mg/L	0.75	R
Unsaturated iron binding capacity	UIBC	11,317	19	0.2±16.6	0.968±0.155	mcg/dL	0.4	R
Sodium	NA	310,234	122,406	−0.19±3.25	0.999±0.023	mmol/L	8	A
Potassium	K+	309,187	119,008	0.026±0.540	1.01±0.14	mmol/L	1	A
Chloride	CL	310,390	122,609	−0.49±4.02	0.996±0.038	mmol/L	8	A
Haptoglobin	HAPTO	727	22	−24.4±22.3	0.853±0.558	mg/dL	–	None
Immunoglobulin A	IGA	4,243	4	26.3±34.5	1.05±0.06	mg/dL	–	None
Immunoglobulin M	IGM	1,944	3	4.3±10.5	1.07±0.12	mg/dL	–	None
Carbamazepine	CARB	974	4	0.370±0.940	1.03±0.10	% COHB	–	None
Digoxin	DGXN	849	16	−0.054±0.438	1.02±0.33	mcg/L	–	None
Immunoglobulin G	IGG	2,353	3	25.0±71	1.037±0.078	mg/dL	–	None
Phenobarbital	PHENOB	415	33	−1.19±4.93	0.968±0.174	mg/L	–	None
Phenytoin	DPH	977	58	−0.50±5.17	0.950±0.329	mg/L	–	None
Theophylline	THEO	61	0	–	–	mg/L	–	None
Lithium	LITH	1,163	13	0.170±0.388	1.49±1.04	mmol/L	0.3	R
Valproic acid	VALP	1,913	47	−3.4±20.3	1.04±0.61	mg/L	–	None
C4 complement	C4	1,573	1	1.00±0	1.06±0	mg/dL	–	None
Prealbumin	PRE ALB	4,152	41	0.71±3.78	1.09±0.33	mg/dL	–	None
Direct low density lipoprotein cholesterol	DLDL	8,400	1	0.00±0	1.00±0	mg/dL	–	None
Urine albumin	UALB	17,694	0	–	–	mg/24 hrs	0.9	R
C3 complement	C3	1,464	1	13.0±0	1.19±0	mg/dL	–	None
Gentamicin peak	GENT P	58	0	–	–	mg/L	–	None
Gentamicin 6–14 hours post-dose	GENT LVL 6 - 14 POST DOSE	29	0	–	–	mg/L	–	None
Gentamicin trough	GENT T	90	2	−0.28±1.80	1.30±1.15	mg/L	–	None
Tobramycin, peak	TOBRA P	34	0	–	–	mg/L	–	None
Tobramycin	TOBRA	182	3	−0.570±0.450	0.481±0.325	mg/L	–	None
Tobramycin, through	TOBRA T	83	0	–	–	mg/L	–	None
Vancomycin, peak	VANC P	34	0	–	–	mg/L	–	None
Vancomycin, trough	VANC T	4,587	78	−0.57±8.45	1.01±0.44	mg/L	–	None
Urine sodium	U NA	2,649	18	−23.2±23.3	0.530±0.350	mmol/L	–	None
Urine potassium	UK	2,561	17	−15.9±35.9	0.941±0.740	mmol/L	–	None
Urine chloride	U CL	2,587	18	−32.1± 37.3	0.543±0.363	mmol/L	–	None
Kappa free light chains	Kap	260	0	–	–	–	–	None
Lambda free light chains	Lam	260	0	–	–	–	–	None
Alpha fetoprotein	AFP	876	0	–	–	ng/mL	–	None
Cyclic citrullinated peptide antibody	CCP	246	0	–	–	U/mL	–	None
Cancer antigen 125	CA 125	309	0	–	–	U/mL	–	None
Carbohydrate antigen 19-9	CA 19-9	125	0	–	–	U/mL	–	None
Dehydroepiandrosterone sulfate	DHEAS	145	0	–	–	mcg/dL	–	None
Homocysteine	Homocyst T	198	0	–	–	mcmol/L	–	None
Insulin	Insulin	144	0	–	–	mcU/mL	–	None
Hepatitis A total antibody	HepA	1	0	–	–		–	None
Hepatitis B surface antibody	HepB sAb	18	0	–	–	IU/L	–	None
Parathyroid hormone	PTH	4,613	12	12.0±40.9	1.18±0.23	pg/mL	–	None
Beta-2-microglobulin	B2MG	44	0	–	–	mg/L	–	None
Alpha 1 antitrypsin	A1AT	285	0	–	–	mg/dL	–	None
Ceruloplasmin	Cerulopl	353	0	–	–	mg/dL	–	None
Free triiodothyronine	Free T3	72	0	–	–	pg/mL	–	None

A, absolute change; N, number; R, relative change; SD, standard deviation.

Table S2 Characterization of training, validation, and testing data sets, along with training parameters, for all neural networks

Neural network type	Δt range (days)	Dataset sizes					Training data		
		Train	Validation	Test	Total	% of specimen pairs	Batches/iteration	Iteration drop	Epochs
PNN-BMP	<1.5	148,480	18,818	18,824	186,122	19.3	300	4	20
PNN-BMP	1.5–2.5	94,830	11,868	11,512	118,210	12.3	300	4	20
PNN-BMP	2.5–3.5	73,594	9,210	9,202	92,006	9.5	300	4	20
PNN-BMP	3.5–5	86,744	10,900	10,932	108,576	11.3	300	4	20
PNN-BMP	5–10	193,874	24,414	24,294	242,582	25.2	300	4	20
PNN-CMP	<1.5	8,014	1,076	1,030	10,120	1.0	40	20	80
PNN-CMP	1.5–2.5	5,378	696	618	6,692	0.7	40	20	80
PNN-CMP	2.5–3.5	4,192	530	498	5,220	0.5	40	20	80
PNN-CMP	3.5–5	4,768	640	622	6,030	0.6	40	20	80
PNN-CMP	5–10	10,810	1,344	1,374	13,528	1.4	40	20	80
PNN-HFP	<1.5	10,404	1,352	1,384	13,140	1.4	40	20	80
PNN-HFP	1.5–2.5	6,664	862	808	8,334	0.9	40	20	80
PNN-HFP	2.5–3.5	5,168	662	638	6,468	0.7	40	20	80
PNN-HFP	3.5–5	5,996	782	816	7,594	0.8	40	20	80
PNN-HFP	5–10	13,906	1,710	1,702	17,318	1.8	40	20	80
PNN-RFP	<1.5	2,050	274	288	2,612	0.3	10	20	100
PNN-RFP	1.5–2.5	1,460	188	152	1,800	0.2	10	20	100
PNN-RFP	2.5–3.5	1,110	168	148	1,426	0.1	10	20	100
PNN-RFP	3.5–5	1,302	188	176	1,666	0.2	10	20	100
PNN-RFP	5–10	2,478	328	284	3,090	0.3	10	20	100
ONN, 5–8 analytes	<1.5	110,236	13,756	13,776	137,768	14.3	100	4	40
ONN, 5–8 analytes	1.5–2.5	66,002	8,226	8,152	82,380	8.5	100	4	40
ONN, 5–8 analytes	2.5–3.5	49,664	6,198	6,284	62,146	6.4	100	4	40
ONN, 5–8 analytes	3.5–5	57,074	7,094	7,174	71,342	7.4	100	4	40
ONN, 5–8 analytes	5–10	124,404	15,522	15,448	155,374	16.1	100	4	40
ONN, 9–12 analytes	<1.5	66,962	8,344	8,622	83,928	8.7	100	4	40
ONN, 9–12 analytes	1.5–2.5	40,824	5,080	4,926	50,830	5.3	100	4	40
ONN, 9–12 analytes	2.5–3.5	32,744	3,986	3,960	40,690	4.2	100	4	40
ONN, 9–12 analytes	3.5–5	39,736	5,040	5,036	49,812	5.2	100	4	40
ONN, 9–12 analytes	5–10	88,750	11,252	11,074	111,076	11.5	100	4	40
ONN, ≥13 analytes	<1.5	22,696	2,914	2,954	28,564	3.0	100	4	40
ONN, ≥13 analytes	1.5–2.5	13,506	1,768	1,638	16,912	1.8	100	4	40
ONN, ≥13 analytes	2.5–3.5	11,296	1,416	1,384	14,096	1.5	100	4	40
ONN, ≥13 analytes	3.5–5	13,796	1,730	1,784	17,310	1.8	100	4	40
ONN, ≥13 analytes	5–10	33,434	4,066	4,178	41,678	4.3	100	4	40

BMP, basic metabolic panel; CMP, complete metabolic panel; HFP, hepatic function panel; ONN, open neural network; PNN, panel neural network; RFP, renal function panel.

Table S3 Area under the curve (AUC) obtained from receiver operator characteristics curve (ROC) analysis

Δt range (days)	PNN AUC				ONN AUC		
	BMP	CMP	HFP	RFP	5–8 analytes	9–12 analytes	≥13 analytes
<1.5	0.966±0.004	0.994±0.001	0.989±0.001	0.943±0.009	0.911±0.012	0.935±0.004	0.964±0.002
1.5–2.5	0.932±0.011	0.980±0.003	0.968±0.002	0.902±0.007	0.870±0.018	0.869±0.008	0.920±0.010
2.5–3.5	0.894±0.018	0.967±0.004	0.950±0.006	0.876±0.020	0.830±0.014	0.833±0.012	0.871±0.013
3.5–5	0.859±0.020	0.953±0.007	0.930±0.006	0.831±0.008	0.802±0.011	0.795±0.014	0.845±0.006
5–10	0.862±0.007	0.954±0.004	0.928±0.005	0.827±0.011	0.805±0.018	0.799±0.018	0.829±0.005

BMP, basic metabolic panel; CMP, complete metabolic panel; HFP, hepatic function panel; ONN, open neural network; PNN, panel neural network; RFP, renal function panel.

Table S4 Panel neural networks (PNN) performance

Panel	Δt range (days)	OOP			Sn set to 0.5			Sn set to 0.8			Classic		
		Sn	Sp	PPV	Sn	Sp	PPV	Sn	Sp	PPV	Sn	Sp	PPV
BMP	<1.5	89.6	91.4	4.9	50.0	99.7	41.7	80.0	96.6	10.7	91.3	74.0	1.7
BMP	1.5–2.5	84.0	87.4	3.2	50.0	98.7	15.9	80.0	90.5	4.0	91.1	57.2	1.1
BMP	2.5–3.5	78.5	83.6	2.3	50.0	97.0	7.6	80.0	81.7	2.1	90.1	47.0	0.8
BMP	3.5–5	75.4	79.3	1.8	50.0	94.9	4.7	80.0	73.9	1.5	91.5	39.8	0.8
BMP	5–10	75.8	80.6	1.9	50.0	94.8	4.6	80.0	75.5	1.6	91.5	31.9	0.7
CMP	<1.5	98.4	96.4	12.1	50.0	99.9	68.1	80.0	99.4	39.2	99.6	61.4	1.3
CMP	1.5–2.5	92.3	94.3	7.5	50.0	100	100	80.0	99.0	28.5	99.0	37.2	0.8
CMP	2.5–3.5	90.8	92.9	6.0	50.0	99.6	36.1	80.0	97.7	14.7	100	26.5	0.7
CMP	3.5–5	86.0	91.4	4.8	50.0	99.7	46.4	80.0	94.2	6.4	99.7	19.3	0.6
CMP	5–10	89.3	88.5	3.7	50.0	99.4	29.0	80.0	93.8	6.1	99.4	20.1	0.6
HFP	<1.5	96.4	95.0	8.9	50.0	99.8	61.1	80.0	99.0	28.1	99.3	61.4	1.3
HFP	1.5–2.5	89.4	92.9	6.0	50.0	99.9	66.8	80.0	97.6	14.4	99.3	37.4	0.8
HFP	2.5–3.5	88.7	89.9	4.2	50.0	99.1	21.6	80.0	94.1	6.4	99.7	26.6	0.7
HFP	3.5–5	84.5	87.1	3.2	50.0	98.8	17.2	80.0	89.5	3.7	99.5	19.1	0.6
HFP	5–10	85.5	84.7	2.7	50.0	98.6	15.5	80.0	88.7	3.4	98.6	21.3	0.6
RFP	<1.5	90.9	85.9	3.1	50.0	97.9	10.7	80.0	91.0	4.2	99.3	59.0	1.2
RFP	1.5–2.5	80.3	89.1	3.5	50.0	98.7	16.0	80.0	85.3	2.6	100	42.1	0.9
RFP	2.5–3.5	84.5	82.0	2.3	50.0	93.2	3.6	80.0	82.7	2.3	100	17.6	0.6
RFP	3.5–5	70.7	83.4	2.1	50.0	94.5	4.4	80.0	68.1	1.2	100	14.8	0.6
RFP	5–10	75.5	75.8	1.5	50.0	91.7	2.9	80.0	66.9	1.2	99.3	7.0	0.5

Sensitivity (Sn), specificity (Sp), and positive predictive values (PPV) are reported in percent (%). BMP, basic metabolic panel; CMP, complete metabolic panel; HFP, hepatic function panel; ONN, open neural network; OOP, optimal operating point; PNN, panel neural network; RFP, renal function panel.

Table S5 Open neural networks (ONN) performance

N analytes (range)	Δt range (days)	OOP			Sn set to 0.5			Se set to 0.8			Classic		
		Sn	Sp	PPV	Sn	Sp	PPV	Sn	Sp	PPV	Sn	Sp	PPV
5–8	<1.5	80.3	84.5	2.5	50.0	97.4	8.7	80.0	84.0	2.4	82.4	78.6	1.9
5–8	1.5–2.5	74.2	81.7	2.0	50.0	94.1	4.1	80.0	75.4	1.6	83.8	62.5	1.1
5–8	2.5–3.5	77.0	72.4	1.4	50.0	91.9	3.0	80.0	67.8	1.2	84.4	52.2	0.9
5–8	3.5–5	69.1	75.5	1.4	50.0	87.9	2.0	80.0	63.7	1.1	84.4	45.9	0.8
5–8	5–10	71.5	73.4	1.3	50.0	88.4	2.1	80.0	63.7	1.1	84.8	40.3	0.7
9–12	<1.5	86.6	84.5	2.7	50.0	99.0	19.7	80.0	90.0	3.8	89.1	68.7	1.4
9–12	1.5–2.5	81.4	75.6	1.6	50.0	95.1	4.9	80.0	76.2	1.7	89.6	53.4	1.0
9–12	2.5–3.5	76.5	73.8	1.4	50.0	92.3	3.1	80.0	68.9	1.3	87.5	45.6	0.8
9–12	3.5–5	71.7	71.1	1.2	50.0	88.5	2.1	80.0	61.2	1.0	88.6	39.7	0.7
9–12	5–10	73.3	70.8	1.2	50.0	89.2	2.3	80.0	62.3	1.0	88.4	30.8	0.6
≥13	<1.5	90.4	88.9	3.9	50.0	99.5	35.5	80.0	95.7	8.5	93.7	64.7	1.3
≥13	1.5–2.5	83.6	85.1	2.7	50.0	98.3	12.7	80.0	87.1	3.0	94.3	44.7	0.8
≥13	2.5–3.5	80.3	77.2	1.7	50.0	95.5	5.2	80.0	76.3	1.7	93.9	34.5	0.7
≥13	3.5–5	74.5	77.5	1.6	50.0	93.3	3.6	80.0	71.0	1.4	93.6	29.1	0.7
≥13	5–10	74.6	73.3	1.4	50.0	91.5	2.9	80.0	66.9	1.2	93.8	26.1	0.6

Sensitivity (Sn), specificity (Sp), and positive predictive values (PPV) are reported in percent (%). BMP, basic metabolic panel; CMP, complete metabolic panel; HFP, hepatic function panel; ONN, open neural network; OOP, optimal operating point; PNN, panel neural network; RFP, renal function panel.